COMPDYN 2011
3rd ECCOMAS Thematic Conference on
Computational Methods in Structural Dynamics and Earthquake Engineering
M. Papadrakakis, M. Fragiadakis, V. Plevris (eds.)
Corfu, Greece, 25–28 May 2011

NONLINEAR DYNAMIC BEHAVIOUR OF A SADDLE FORM CABLE NET MODELED BY AN EQUIVALENT SDOF CABLE NET

Isabella Vassilopoulou and Charis J. Gantes

Metal Structures Laboratory, National Technical University of Athens
9 Iroon Polytechniou, GR-15780 Zografou - Athens, Greece
isabella@central.ntua.gr, chgantes@central.ntua.gr

Keywords: equivalent SDOF model, saddle form cable net, nonlinear dynamic response, similarity relations.

Abstract. *The purpose of this paper is to estimate the geometrically nonlinear dynamic behavior of a saddle form cable net, using an equivalent single-degree-of-freedom model. First, a symmetric simple cable net is assumed, consisting of two crossing cables, considering the vertical displacement of the central node as the only degree of freedom. The equation of motion is found to be similar to the one of the Duffing oscillator with a hardening cubic term. Next, a MDOF symmetric cable net model is considered, with fixed cable ends, having a circular plan view and forming a surface of a hyperbolic paraboloid. Harmonic external loads act vertically on every node of the net, with the same amplitude and time variation. Modal analyses are conducted in order to calculate the linear eigenfrequencies and the corresponding eigenmodes of the network. The nonlinear dynamic response of the cable net is obtained by performing time history analysis. Detecting nonlinear phenomena, such as bending of the response curve, jump phenomena, different response amplitudes according to the initial conditions, superharmonic or subharmonic resonances, demands much computational effort for different load amplitudes and ratios of loading frequency. Based on a method of approximate analysis for prediction of the response of cable nets, the MDOF model is transformed to an equivalent SDOF one, using similarity relations. The analytical solution of the single-degree-of-freedom model can provide, with minimum computational time, the basic information needed for nonlinear dynamic response, i.e. secondary resonances, jump phenomena, dependence on the initial conditions and the exact loading frequency for which the maximum steady state oscillation amplitude is obtained. The comparison between the two models by means of the steady state amplitude of the central node, demonstrates that the behavior of the SDOF model describes satisfactorily the one of the MDOF model, predicting the dominant nonlinear phenomena.*

1 INTRODUCTION

Nonlinear phenomena, such as superharmonic or subharmonic resonances, bending of the response curve and jump phenomena, as well as response amplitudes dependent on the initial conditions, that occur in nonlinear systems [1], are very difficult to be detected in a multi-degree-of-freedom system. The only way to plot a response curve, which can show if the above phenomena take place, is by conducting a large number of nonlinear time history analyses, for different closely spaced load amplitudes and frequencies, but this is a time consuming procedure requiring much computation effort.

The idea of solving an equivalent SDOF system to estimate the dynamic response of a complex structure has been adopted by many researchers ([2]-[9]). This idea is based on equating the energy of the real structure to the one of the SDOF system. Ensuring equal displacements and velocities in both systems, the kinematic similarity is maintained. This approach has the advantage that the equation of motion for a SDOF oscillator can be solved analytically. Hence, it is possible to determine the range of the parameters that influence the dynamic response of the system. On the other hand, it is impossible to assess the overall response of the MDOF system, because the simulation is obtained only in the main direction of motion, neglecting the other two dimensions of the large structure.

Another method of reducing the dimensions of a large scale event, using a smaller one with similar characteristics, is a method based on the Buckingham Pi theorem [10]. This theorem states that if an equation involves a number of variables and k fundamental measurement units, then the equation can be expressed in terms of k fewer arguments that are non-dimensional ratios of the original variables. The concept is based on the notion that an equation must be dimensionally homogeneous, that is, its solution must be invariant to any change in the system of measurement units employed. This technique has been used to design small scale experiments in order to simulate with accuracy large scale phenomena.

Gero ([11], [12]), inspired by this theorem, presented a method to estimate the static behaviour of a large cable net, using charts that describe the behaviour of a smaller one, by means of the maximum deflection and cable tension. The transformation of the large structure to the smaller one was obtained by similarity relations. The proposed method was restricted to nets with fixed cable edges. The two networks should have similar geometries, with the same sag-to-span ratio, so that their corresponding quantities could also be similar.

This latter method was extended by the authors of the present paper to elastically supported cable network structures, by taking into account the characteristics of the edge ring, and more specifically its flexural stiffness E_rI_r ([13] - [15]). Thus, the ring was no longer considered rigid, but elastically deformable, accounting for more realistic boundary conditions for the cables. Additional charts and similarity relations were provided for the preliminary design of the edge ring, including the sag-to-span ratio of the net as a variable in the transformation relations. This method was further developed for the case of dynamic response [16], providing additional similarity relations for the mass and the natural frequency of the system, for the case of fixed cable ends.

This preliminary design method is used in the present work to transform a MDOF cable net, called prototype, into an equivalent SDOF cable net, called model, in order to solve analytically the equation of motion, and thus have the possibility to detect nonlinear phenomena and estimate the nonlinear dynamic response of the large structure. The analytical solution, which plots the steady state amplitude of the equivalent SDOF model, is compared with the steady state response of the MDOF system, obtained numerically. The accuracy of the method is evaluated by means of a numerical example.

2 PROTOTYPE AND MODEL ASSUMPTIONS

The cable net used as prototype, has a diameter L_p=100m and sag-to-span ratio equal to f_p/L_p=1/35 (f_p=2.857m), while the number of cables in each direction is N_p=25 (Figure 1). The Young modulus is assumed equal to E_p=165GPa. The unit weight of the cables is taken equal to ρ_p=100kN/m^3, which corresponds to a concentrated mass on every node equal to:

$$M_p = \frac{2A_p\rho_p L_p}{g(N_p+1)} = 0.151\,\text{kN}\,\text{sec}^2\,\text{m}^{-1} \quad (1)$$

Uniform harmonic loads, expressed as $P_p(t)=(P_0)_p\cos\Omega_p t$, are assumed to be exerted vertically on every node of the net, having the same amplitude and time variation. The maximum permissible cable stress is assumed equal to the yield stress of the material. In this work the yield stress is assumed equal to 1570MPa considering one of the two most common categories of steel for cables 1570/1770MPa. The oscillation of the central node of the net will be used to describe the response of the net. Raleigh damping [17] is also introduced taking into account damping ratio equal to ζ_p=2%, which is a common value for such structures [18]. The subscript p refers to the prototype.

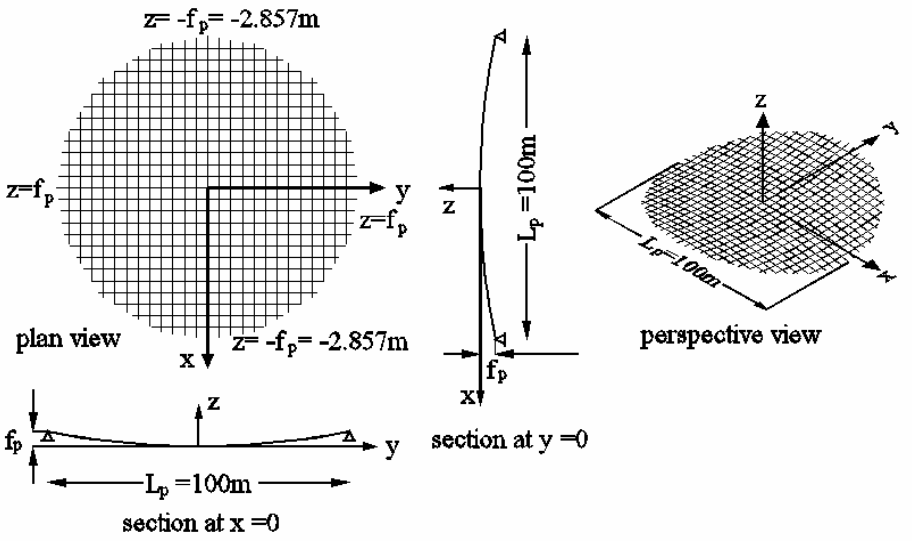

Figure 1: Geometry of the prototype

The model utilized as the equivalent SDOF system consists of two crossing cables (N_m=1), with a concentrated mass at the central node M_m. In order to minimize the scaling error, the model has the same sag-to-span ratio f_m/L_m, cable span L_m, and Young modulus E_m with the prototype. A harmonic load, expressed as $P_m(t)=(P_0)_m\cos\Omega_m t$, is exerted vertically on the central node (Figure 2). The subscript m refers to the model.

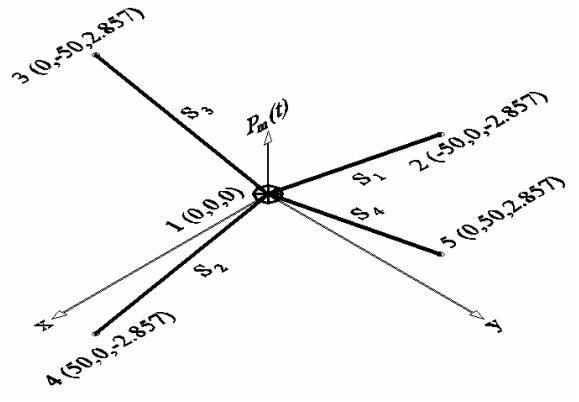

Figure 2: Geometry of the model

3 SIMILARITY RELATIONS

The relations that are used in this work for the transformation of the large cable net (prototype), to the simple one (model), are based on the ones given in [16], for a cable net with fixed cable ends. Taking into account that the sag-to-span ratio, the cable span and the Young modulus are the same for both the prototype and the model, the similarity relations that will be used are the following:

$$(P_0)_m = (P_0)_p \left(\frac{N_p + 1}{N_m + 1} \right)^2 \quad \text{: nodal load amplitude} \tag{2}$$

$$D_m = D_p \sqrt{\left(\frac{N_p + 1}{N_m + 1} \right)} \quad \text{: cable diameter} \tag{3}$$

$$A_m = A_p \left(\frac{N_p + 1}{N_m + 1} \right) \quad \text{: cable cross-sectional area} \tag{4}$$

$$(EA)_m = (EA)_p \left(\frac{N_p + 1}{N_m + 1} \right) \quad \text{: cable axial stiffness} \tag{5}$$

$$(N_0)_m = (N_0)_p \left(\frac{N_p + 1}{N_m + 1} \right) \quad \text{: cable initial pretension} \tag{6}$$

$$M_m = M_p \left(\frac{N_p + 1}{N_m + 1} \right)^2 \quad \text{: nodal mass} \tag{7}$$

$w_m = w_p$: nodal deflection (8)

$\omega_m = \omega_p$: natural frequency (9)

where N is the number of cables per direction and E the elastic modulus of the cables, while the subscripts m and p refer to the model and the prototype, respectively. Two more relations are added, describing the loading frequency and the damping ratio:

$\Omega_m = \Omega_p = \Omega$: loading frequency (10)

$\zeta_m = \zeta_p = \zeta$: damping ratio (11)

4 ANALYTICAL SOLUTION FOR THE MODEL

4.1 Equation of motion

In this section, the analytical equation of motion of the simple cable net, which consists the model of the method, is derived. The initial pretension is introduced as initial elongation $\varepsilon_{0,m}$ to all cable segments, which, according to Hook's law, is equal to:

$$(N_0)_m = (EA)_m \varepsilon_{0,m} \tag{12}$$

S_N is the length of each segment at the equilibrium state under pretension, given as:

$$S_N = \sqrt{(L_m/2)^2 + f_m^2} \tag{13}$$

The initial length S_0 for all segments is equal to:

$$\frac{S_N - S_0}{S_0} = \varepsilon_{0,m} \Rightarrow S_0 = \frac{S_N}{1+\varepsilon_{0,m}} = \frac{S_N}{1+\dfrac{(N_0)_m}{(EA)_m}} \tag{14}$$

If the vertical displacement of the central node is defined as w_m, the deformed lengths of the cable segments are given as:

$$S_{1,2} = \sqrt{(L_m/2)^2 + (f_m + w_m)^2}\ ,\ S_{3,4} = \sqrt{(L_m/2)^2 + (f_m - w_m)^2} \tag{15}$$

The cable tension for each deformed segment is expressed as:

$$(N_i)_m = (EA)\left(\frac{S_i - S_0}{S_0}\right) = (N_0)_m + (EA)_m\left(\frac{S_i - S_N}{S_0}\right),\ i=1,2,3,4 \tag{16}$$

Their components, referring to the global axes, are calculated as:

$$(N_{1,2x})_m=(N_{1,2})_m\cdot(L_m/2)/(S_{1,2}),\quad (N_{1,2z})_m= \pm(N_{1,2})_m\cdot(f_m+w_m)/(S_{1,2})$$
$$(N_{3,4y})_m=(N_{3,4})_m\cdot(L_m/2)/(S_{3,4}),\quad (N_{3,4z})_m= \pm(N_{3,4})_m\cdot(w_m-f_m)/(S_{3,4}) \tag{17}$$

The sum of forces at the central node, referring to the x, y, z global axes, are:

$$(N_x)_m=(N_y)_m=0,\qquad (N_z)_m=(N_{1z})_m - (N_{2z})_m + (N_{3z})_m - (N_{4z})_m \tag{18}$$

Differentiating Eq. (18) with respect to w_m, and considering zero displacement for the unforced and undeformed state, the stiffness coefficient at the prestressed equilibrium state is:

$$K_m = \frac{4(EA)_m}{L_m}\cdot\frac{\left(8\dfrac{f_m^2}{L_m^2} + 2\dfrac{(N_0)_m}{(EA)_m} + 8\dfrac{(N_0)_m}{(EA)_m}\dfrac{f_m^2}{L_m^2}\right)}{\sqrt{\left(1+4\dfrac{f_m^2}{L_m^2}\right)^3}} \tag{19}$$

In case a dynamic vertical load $P_m(t)$ is applied on the central node, the equation of motion of this node is expressed in the equilibrium state:

$$M_m\ddot{w}_m + C\dot{w}_m + (N_{1z})_m - (N_{2z})_m + (N_{3z})_m - (N_{4z})_m = P_m(t) \tag{20}$$

The damping C is a function of the damping ratio ζ, expressed as [17]:

$$C=\zeta\cdot C_{cr}=2\zeta M_m\omega_m \tag{21}$$

where ω_m is the natural frequency of the system.

If the dynamic load is expressed as $P_m(t)=(P_0)_m\cos\Omega t$, substituting the expressions of the tension of the cables, given by Eq. (16) and the prestressed, initial and deformed lengths, given by Eqs. (13) - (15), into the vertical components of the cable tensions (Eq. (17)), the differential equation (20) becomes:

$$\begin{aligned} &M_m\ddot{w}_m + C\dot{w}_m - \frac{4(EA)_m(f_m+w_m)}{L_m\sqrt{1+4\dfrac{(f_m+w_m)^2}{L_m^2}}} + \\ &+\frac{4(EA)_m(f_m-w_m)}{L_m\sqrt{1+4\dfrac{(f_m-w_m)^2}{L_m^2}}} + \frac{4w_m\left((EA)_m+(N_0)_m\right)}{L_m\sqrt{1+4\dfrac{f_m^2}{L_m^2}}} = P_m(t) \end{aligned} \tag{22}$$

Taking into account that the sag-to-span ratio f/L is usually very small for actual cable nets, allowing thus to neglect its second, third or higher powers, Eq. (22), developed in Taylor series, reduces to:

$$\begin{aligned} &M_m\ddot{w}_m + C\dot{w}_m + \frac{16(EA)_m w_m^3}{L_m^3} + \\ &+\frac{4(EA)_m}{L_m}\cdot\left(8\frac{f_m^2}{L_m^2}+2\frac{(N_0)_m}{(EA)_m}-4\frac{N_0)_m}{(EA)_m}\frac{f_m^2}{L_m^2}\right)w_m = P_m(t) \end{aligned} \tag{23}$$

Expanding the expression of the stiffness K_m, given by Eq. (19), in Taylor series with respect to the term f/L and neglecting terms of $(f/L)^4$, leads to:

$$K_m = \frac{4(EA)_m}{L_m}\cdot\left(8\frac{f_m^2}{L_m^2}+2\frac{(N_0)_m}{(EA)_m}-4\frac{(N_0)_m}{(EA)_m}\frac{f_m^2}{L_m^2}\right) \tag{24}$$

Thus, Eq. (23) can be rewritten as:

$$\ddot{w}_m + \frac{C}{M_m}\dot{w}_m + \frac{K_m}{M_m}w_m + \frac{16(EA)_m}{M_mL_m^3}w_m^3 = \frac{(P_0)_m}{M_m}\cos(\Omega t) \tag{25}$$

where a nonlinear cubic term appears with a coefficient depending on the modulus of elasticity of the cable material, the cable cross-section area and the span of the cables.

Nayfeh and Mook [19] thoroughly explored the equation:

$$\ddot{w} + 2\varepsilon\mu\dot{w} + \omega_0^2 w + \varepsilon\alpha w^3 = K\cos(\Omega t) \tag{26}$$

known as the equation of motion referring to a forced damped Duffing oscillator, with μ being positive, and the coefficient of the nonlinear term α being either positive (hard spring) or negative (soft spring). The equation of motion of the simple cable net, described by Eq. (25), can take the form of Eq. (26), with positive coefficient of the nonlinear term and become:

$$\ddot{w}_m + 2\varepsilon\mu\dot{w}_m + \omega_m^2 w_m + \varepsilon\alpha w_m^3 = p_m\cos(\Omega t) \tag{27}$$

where:

$$\varepsilon\mu=\zeta\omega_m \tag{28}$$

$$\omega_m = \sqrt{\frac{4(EA)_m}{M_m L_m} \cdot \left(8\frac{f_m^2}{L_m^2} + 2\frac{(N_0)_m}{(EA)_m} - 4\frac{(N_0)_m}{(EA)_m}\frac{f_m^2}{L_m^2} \right)} \tag{29}$$

$$\varepsilon\alpha = \frac{16(EA)_m}{M_m L_m^3} \tag{30}$$

$$p_m = \frac{(P_0)_m}{M_m} \tag{31}$$

The parameter ε is assumed to be small and dimensionless, with ε<1, defining the small scale of the coefficients of the velocity and the cubic term in the equation of motion with respect to the one of the linear term. The exact value of this parameter is not important, because the solution of the problem is independent of ε. It depends only on the parameters εμ and εα, as defined in Eqs. (28) and (30), respectively, meaning that the parameter ε never appears alone in the solution. In what follows the main features of the investigation of the Duffing oscillator are reported from [19].

4.2 Fundamental resonance

In case of fundamental resonance the excitation is assumed to be weak, in order to prove that a weak excitation produces large scale oscillations. The small amplitude of the load is expressed as:

$$\varepsilon p = \frac{(P_0)_m}{M_m} \tag{32}$$

For fundamental resonant conditions, the steady state response is given as:

$$w(t) = a\cos(\Omega t - \gamma) \tag{33}$$

where Ω is the loading frequency expressed as:

$$\Omega = \omega_m + \varepsilon\sigma \tag{34}$$

with εσ a frequency detuning, which, for a given amplitude of the response, is calculated by the following equation:

$$\sigma = \frac{3\alpha a^2}{8\omega_m} \pm \sqrt{\frac{p^2}{4\omega_m^2 a^2} - \mu^2} \Rightarrow \varepsilon\sigma = \frac{3\varepsilon\alpha a^2}{8\omega_m} \pm \sqrt{\frac{(\varepsilon p)^2}{4\omega_m^2 a^2} - (\varepsilon\mu)^2} \tag{35}$$

Taking into consideration Eqs. (28), (30) and (32), Eq. (35) can be rewritten as:

$$\varepsilon\sigma = \frac{6a^2}{\omega_m} \cdot \frac{(EA)_m}{M_m L_m^3} \pm \sqrt{\frac{(P_0)_m^2}{4M_m^2\omega_m^2 a^2} - (\zeta\omega_m)^2} \tag{36}$$

4.3 Superharmonic resonance

For superharmonic resonant conditions, the steady state response is given as:

$$w(t) = a\cos(3\Omega t - \gamma) + \frac{(P_0)_m}{M_m}\left(\frac{1}{\omega_m^2 - \Omega^2}\right)\cos\Omega t \tag{37}$$

The loading frequency is expressed as:

$$3\Omega=\omega_m+\varepsilon\sigma \tag{38}$$

For a given amplitude of the free oscillation term a, the frequency detuning is calculated by:

$$\begin{aligned}
&\sigma=\frac{3\alpha\Lambda^2}{\omega_m}+\frac{3\alpha a^2}{8\omega_m}\pm\sqrt{\frac{\alpha^2\Lambda^6}{\omega_m^2 a^2}-\mu^2}\Rightarrow\\
&\Rightarrow\varepsilon\sigma=\frac{48\Lambda^2}{\omega_m}\cdot\frac{(EA)_m}{M_m L_m^3}+\frac{6a^2}{\omega_m}\cdot\frac{(EA)_m}{M_m L_m^3}\pm\sqrt{\frac{\Lambda^6}{\omega_m^2 a^2}\cdot\left(\frac{16(EA)_m}{M_m L_m^3}\right)^2-(\zeta\omega_m)^2}
\end{aligned} \tag{39}$$

where

$$\Lambda=\frac{(P_0)_m}{2M_m}\left(\frac{1}{\omega_m^2-\Omega^2}\right) \tag{40}$$

4.4 Subharmonic resonance

In case of subharmonic resonance, the loading frequency is expressed as:

$$\Omega=3\omega_m+\varepsilon\sigma \tag{41}$$

For a given detuning $\varepsilon\sigma$, subharmonic solutions with non trivial amplitudes ($a\neq 0$) exist only if:

$$\begin{aligned}
&\frac{\sigma}{\mu}-\sqrt{\frac{\sigma^2}{\mu^2}-63}\le\frac{63\alpha}{4\omega_{z0}\mu}\Lambda^2\le\frac{\sigma}{\mu}+\sqrt{\frac{\sigma^2}{\mu^2}-63}\Rightarrow\\
&\frac{\varepsilon\sigma}{\zeta\omega_m}-\sqrt{\frac{(\varepsilon\sigma)^2}{(\zeta\omega_m)^2}-63}\le\frac{256\Lambda^2}{\zeta\omega_m^2}\cdot\frac{(EA)_m}{M_m L_m^3}\le\frac{\varepsilon\sigma}{\zeta\omega_m}+\sqrt{\frac{(\varepsilon\sigma)^2}{(\zeta\omega_m)^2}-63}
\end{aligned} \tag{42}$$

where Λ is given by Eq. (40), while for a given Λ subharmonic solution with non trivial amplitudes ($a\neq 0$) exist if:

$$\sigma\ge\frac{63\alpha}{8\omega_m}\Lambda^2+\frac{2\omega_m}{\alpha}\frac{\mu^2}{\Lambda^2}\Rightarrow\varepsilon\sigma\ge\frac{126\Lambda^2}{\omega_m}\cdot\frac{(EA)_m}{M_m L_m^3}+\frac{M_m L_m^3}{8(EA)_m}\frac{\zeta^2\omega_m^3}{\Lambda^2} \tag{43}$$

with amplitude given by:

$$\begin{aligned}
&a^2=\left(\sigma\frac{8\omega_m}{9\alpha}-6\Lambda^2\right)\pm\sqrt{\left(\sigma\frac{8\omega_m}{9\alpha}-6\Lambda^2\right)^2-\frac{64\omega_m^2}{81\alpha^2}\left[\left(\sigma-\frac{9\alpha\Lambda^2}{\omega_m}\right)^2+9\mu^2\right]}\Rightarrow\\
&\Rightarrow a^2=\left(\varepsilon\sigma\frac{\omega_m M_m L_m^3}{18(EA)_m}-6\Lambda^2\right)\pm\\
&\pm\sqrt{\left(\varepsilon\sigma\frac{\omega_m M_m L_m^3}{18(EA)_m}-6\Lambda^2\right)^2-\frac{M_m^2 L_m^6\omega_m^2}{324(EA)_m^2}\left[\left(\varepsilon\sigma-\frac{9\Lambda^2}{\omega_m}\cdot\frac{16(EA)_m}{M_m L_m^3}\right)^2+9(\zeta\omega_m)^2\right]}
\end{aligned} \tag{44}$$

In case no subharmonic resonant conditions exist, the steady-state response depends only on the external load:

$$w(t) = \frac{(P_0)_m}{M_m}\left(\frac{1}{\omega_m^2 - \Omega^2}\right)\cos\Omega t \tag{45}$$

while, for the non trivial stable solution of a ($a \neq 0$), the response of the nonlinear system at steady-state is:

$$w(t) = a\cos\left(\frac{\Omega t - \gamma_0}{3}\right) + \frac{(P_0)_m}{M_m}\left(\frac{1}{\omega_m^2 - \Omega^2}\right)\cos\Omega t \tag{46}$$

5 NUMERICAL EXAMPLE 1

A numerical example is used in order to explain the method. For this example, the cable diameter of the prototype is assumed equal to D_p=50mm, with a cross-sectional area A_p=0.00196m^2. Approximating realistic structures, the initial cable pretension is $(N_0)_p$=600kN, which corresponds to 19% of the yield stress, considering yield stress 1570MPa.

5.1 Transformation of the prototype to the model

Using the similarity relations, the equivalent SDOF model has the following characteristics:

$$D_m = D_p\sqrt{\left(\frac{N_p + 1}{N_m + 1}\right)} = 0.05\sqrt{\left(\frac{26}{2}\right)} = 0.18\text{m} \tag{47}$$

$$A_m = A_p\left(\frac{N_p + 1}{N_m + 1}\right) = 0.00196 \cdot \frac{26}{2} = 0.0255\text{m}^2 \tag{48}$$

$$(EA)_m = (EA)_p\left(\frac{N_p + 1}{N_m + 1}\right) = 165000000 \cdot 0.0255 = 4211697.6\text{kN} \tag{49}$$

$$(N_0)_m = (N_0)_p\left(\frac{N_p + 1}{N_m + 1}\right) = 600\frac{26}{2} = 7800\text{kN} \tag{50}$$

$$M_m = M_p\left(\frac{N_p + 1}{N_m + 1}\right)^2 = 0.151 \cdot \left(\frac{26}{2}\right)^2 = 25.52\text{kN}\sec^2\text{ m}^{-1} \tag{51}$$

5.2 Analytical solution for the SDOF model

5.2.1. Eigenfrequency of the model

The eigenfrequency of the SDOF model is calculated by Eq. (29):

$$\omega_m = 8.22\sec^{-1} \tag{52}$$

5.2.2. Fundamental resonance

A load amplitude is chosen for the prototype equal to $(P_0)_p$=1.30kN, corresponding to a nodal load for the SDOF model, equal to:

$$(P_0)_m = (P_0)_p \left(\frac{N_p + 1}{N_m + 1} \right)^2 = 1.30 \cdot \left(\frac{26}{2} \right)^2 = 219.70\text{kN} \tag{53}$$

The load amplitude is chosen large enough to cause nonlinear phenomena, without cable tensile failure. The response curve is based on Eq. (36):

$$\varepsilon\sigma = \frac{6a^2}{\omega_m} \cdot \frac{(EA)_m}{M_m L_m^3} \pm \sqrt{\frac{(P_0)_m^2}{4M_m^2 \omega_m^2 a^2} - (\zeta\omega_m)^2} = \left(0.12a^2 \pm \sqrt{\frac{0.27}{a^2} - 0.027} \right) \text{sec}^{-1} \tag{54}$$

while the frequency ratio is calculated as:

$$\frac{\Omega}{\omega_m} = \frac{\omega_m + \varepsilon\sigma}{\omega_m} \tag{55}$$

The amplitude of the steady state response, given by Eq. (54), with respect to the ratio of the loading frequency over the eigenfrequency, is plotted in Figure 3. The bending of the curve indicates the intense nonlinearity of the system. This bending means that jump phenomena are expected to characterize the response of the prototype, multiple response amplitudes dependent on the initial conditions, while the maximum steady state amplitude is predicted for frequency ratio larger than 1.

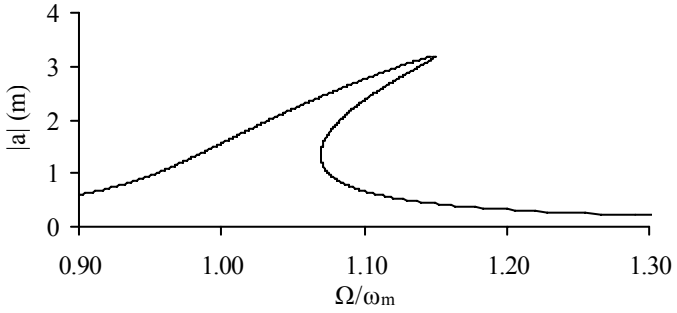

Figure 3: Fundamental resonance: response curve of the SDOF model for load amplitude $(P_0)_m$=219.70kN

5.2.3. Superharmonic resonance

A load amplitude is chosen for the prototype equal to $(P_0)_p$=14kN, corresponding to a nodal load for the SDOF model, equal to:

$$(P_0)_m = (P_0)_p \left(\frac{N_p + 1}{N_m + 1} \right)^2 = 14 \cdot \left(\frac{26}{2} \right)^2 = 2366\text{kN} \tag{56}$$

meaning:

$$\Lambda = \frac{(P_0)_m}{2 \cdot M_m} \left(\frac{1}{\omega_m^2 - \Omega^2} \right) = 0.772\text{m} \tag{57}$$

Again, the load amplitude is chosen large enough to cause nonlinear phenomena, without cable tensile failure. The diagram of the steady state response is defined by Eq. (39):

$$\varepsilon\sigma = \frac{48\Lambda^2}{\omega_m}\cdot\frac{(EA)_m}{M_m L_m^3} + \frac{6a^2}{\omega_m}\cdot\frac{(EA)_m}{M_m L_m^3} \pm \sqrt{\frac{\Lambda^6}{\omega_m^2 a^2}\cdot\left(\frac{16(EA)_m}{M_m L_m^3}\right)^2 - (\zeta\omega_m)^2} \Rightarrow$$
$$\varepsilon\sigma = 0.574\,\sec^{-1} + 0.12a^2(\sec^{-1}) \pm \sqrt{\frac{0.022}{a^2}(\sec^{-2}) - 0.027(\sec^{-2})} \quad (58)$$

and the frequency detuning is calculated for a given response amplitude. The total response amplitude is given as:

$$w_m = a + 2\Lambda \quad (59)$$

where Λ this time is calculated as:

$$\Lambda = \frac{(P_0)_m}{2\cdot M_m}\left(\frac{1}{\omega_m^2 - \Omega^2}\right) = \frac{46.36\text{m}/\sec^2}{(8.22\sec^{-1})^2 - \Omega^2} \quad (60)$$

with

$$\Omega = \frac{\omega_m + \varepsilon\sigma}{3} \quad (61)$$

The response diagram, based on Eq. (58), is plotted in Figure 4.

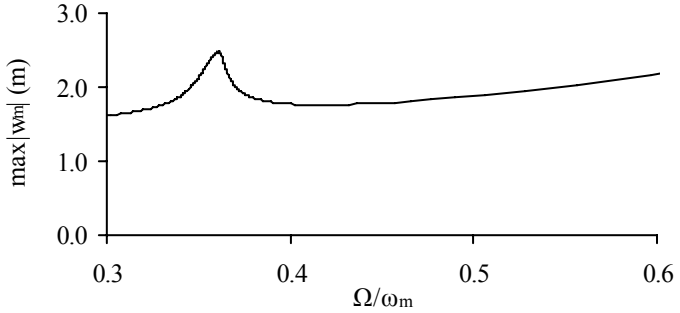

Figure 4: Superharmonic resonance: response curve of the SDOF model for load amplitude $(P_0)_m$=2366kN

5.2.4. Subharmonic resonance

As explained in section 4.4, subharmonic solutions, with non trivial amplitudes of the free oscillation term a, exist for a given value of Λ only if:

$$\varepsilon\sigma \geq \frac{126\Lambda^2}{\omega_m}\cdot\frac{(EA)_m}{M_m L_m^3} + \frac{M_m L_m^3}{8(EA)_m}\cdot\frac{\zeta^2\omega_m^3}{\Lambda^2} \Rightarrow \varepsilon\sigma \geq 2.53\Lambda^2(\sec^{-1}) + \frac{0.168}{\Lambda^2}(\sec^{-1}) \quad (62)$$

Based on Eq. (40) and assuming that:

$$\Omega = 3\omega_m + \varepsilon\sigma \quad (63)$$

the load amplitude is calculated:

$$(P_0)_m = 2M_m\Lambda(\omega_m^2 - \Omega^2) \quad (64)$$

for a frequency detuning satisfying inequality (62), while the amplitude of the oscillation is calculated by Eq. (44):

$$a^2 = \varepsilon\sigma \frac{\omega_m M_m L_m^3}{18(EA)_m} - 6\Lambda^2 \pm$$

$$\pm \sqrt{\left(\varepsilon\sigma \frac{\omega_m M_m L_m^3}{18(EA)_m} - 6\Lambda^2\right)^2 - \frac{M_m^2 L_m^6 \omega_m^2}{324(EA)_m^2}\left[\left(\varepsilon\sigma - \frac{9\Lambda^2}{\omega_m} \cdot \frac{16(EA)_m}{M_m L_m^3}\right)^2 + 9(\zeta\omega_m)^2\right]} \Rightarrow \quad (65)$$

$$a^2 = c \pm \sqrt{c^2 - d \cdot e}$$

where

$$c = (2.77\varepsilon\sigma - 6\Lambda^2)(m^2) \quad (66)$$

$$d = 7.66 m^4 \sec^2 \quad (67)$$

$$e = [(\varepsilon\sigma - 2.89\Lambda^2)^2 + 0.24](\sec^{-2}) \quad (68)$$

Thus, Eq. (65) becomes:

$$a^2 = (2.77\varepsilon\sigma - 6\Lambda^2)(m^2) \pm \\ \pm \sqrt{[(2.77\varepsilon\sigma - 6\Lambda^2)(m^2)]^2 - 7.66 \cdot [(\varepsilon\sigma - 2.89\Lambda^2)^2 + 0.24](m^4)} \quad (69)$$

Figure 5 illustrates the curve that defines the region of the subharmonic solutions, by means of Λ and $(P_0)_m$ with respect to the frequency ratio and to the response amplitude, given by Eq. (69). A detail of the same diagrams is given in Figure 6, for frequency ratio up to 4. In Figure 7 the response amplitude is plotted with respect to the frequency ratio and the loading amplitude. In Figure 8 the detail of the same diagrams is given for frequency ratio up to 4.

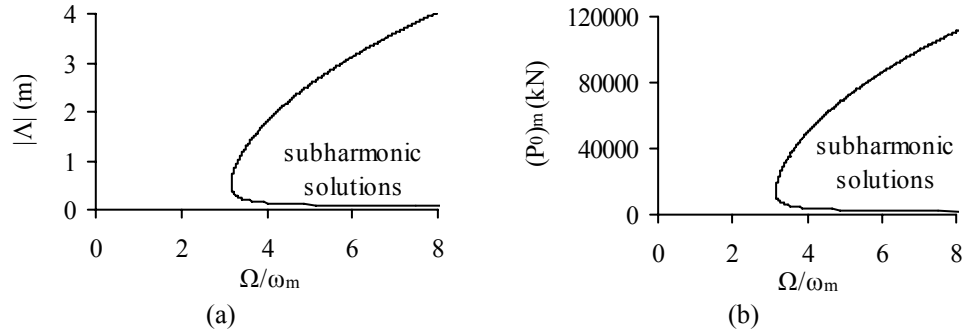

Figure 5: Subharmonic resonance of the SDOF model: a) Λ vs frequency ratio, b) $(P_0)_m$ vs frequency ratio

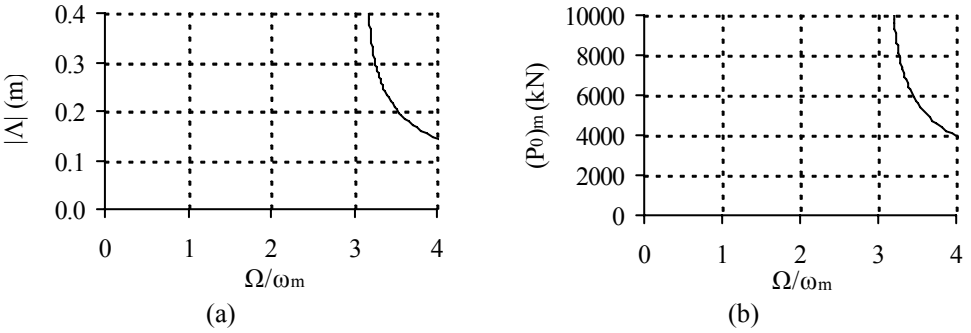

Figure 6: Subharmonic resonance of the SDOF model (detail): a) Λ vs frequency ratio, b) $(P_0)_m$ vs frequency ratio

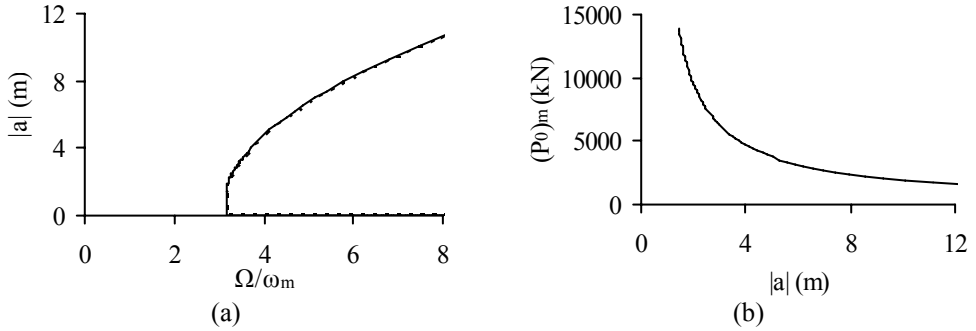

Figure 7: Subharmonic resonance of the SDOF model: a) Response amplitude a vs frequency ratio, b) Load amplitude $(P_0)_m$ vs response amplitude a

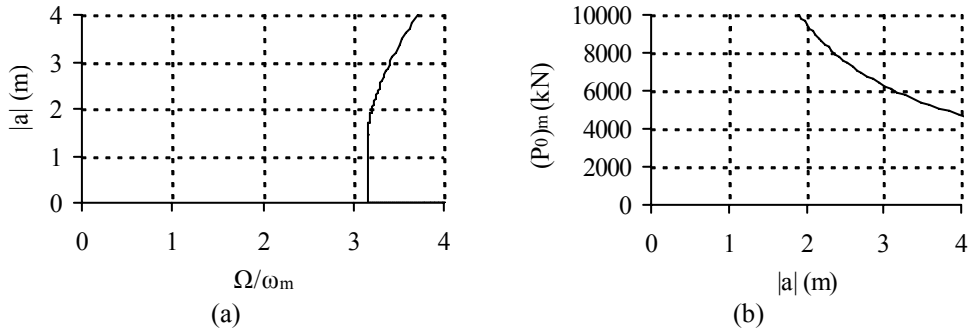

Figure 8: Subharmonic resonance of the SDOF model (detail): a) Response amplitude a vs frequency ratio, b) Load amplitude $(P_0)_m$ vs response amplitude a

The frequency ratios that could cause subharmonic resonance are larger than 3.15 with load amplitude larger than 5239kN, which corresponds to 31kN for the MDOF prototype. A parametric analysis, changing the load amplitude, the frequency ratio and the initial deflection, keeping the initial velocity of the central node equal to 16m/sec, showed that as the load amplitude increases, the minimum initial deflection $w_{0,m}$ and the frequency ratio that can cause subharmonic resonance decrease (Figure 9).

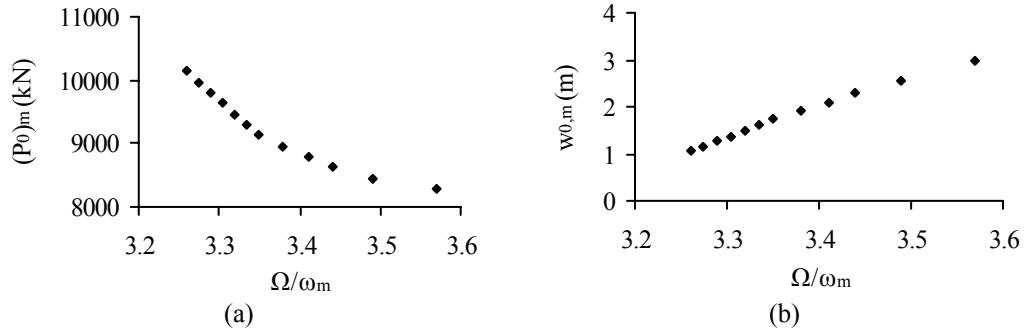

Figure 9: Subharmonic resonant conditions for the SDOF model: a) $(P_0)_m$ vs frequency ratio, b) initial deflection vs frequency ratio

If, for example, the load amplitude is equal to $(P_0)_m$=9464kN, which corresponds to a load amplitude $(P_0)_p$=56kN for the MDOF prototype, the minimum initial deflection required in order to have a subharmonic resonance is 1.49m with a loading frequency equal to $\Omega=3.32\omega_m$, taking into account an initial velocity equal to 16m/sec. The time history diagrams of the central node deflection, for these initial conditions and for null initial conditions, are shown in Figure 10, based on the results obtained by solving numerically the analytical equation of

motion, given by Eq. (25). For a load amplitude equal to $(P_0)_m$=8619kN, corresponding to 51kN for the MDOF prototype, an initial velocity 16m/sec, a minimum initial deflection 2.28m and a loading frequency $\Omega=3.44\omega_m$ constitute the conditions for subharmonic resonance. The time history diagrams of the central node deflection, for these initial conditions and for null initial conditions, are shown in Figure 11.

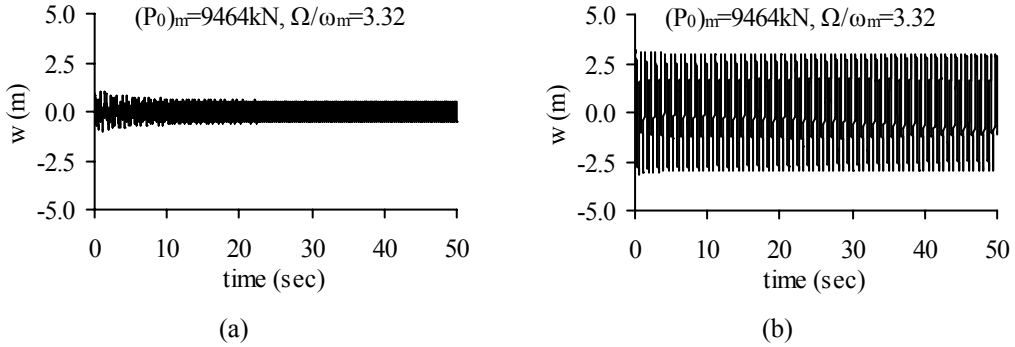

Figure 10: Time history diagrams of the central node deflection for Ω/ω_m=3.32 and $(P_0)_m$=9464kN: a) with null initial conditions, b) with initial displacement and velocity

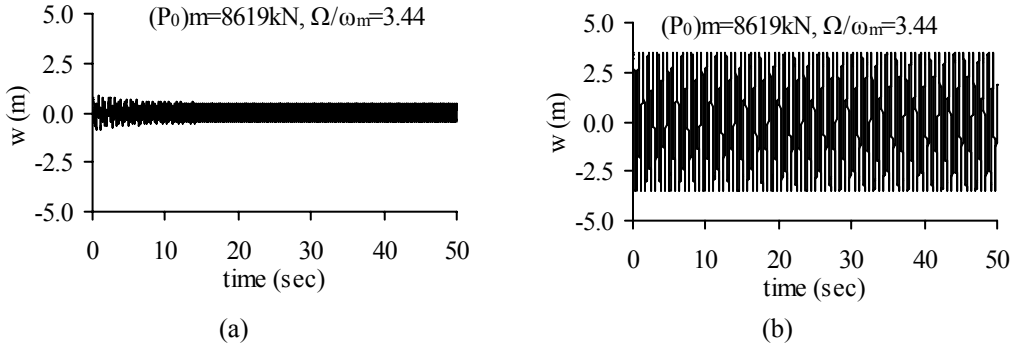

Figure 11: Time history diagrams of the central node deflection for Ω/ω_m=3.44 and $(P_0)_m$=8619kN: a) with null initial conditions, b) with initial displacement and velocity

5.3 Numerical results for the MDOF prototype

In order to evaluate the accuracy of this method, numerical analyses are conducted to estimate the dynamic response of the MDOF cable net, being the prototype for this example.

5.3.1. Eigenfrequencies and eigenmodes of the prototype

A modal analysis is performed to calculate the vibration modes and the natural frequencies of the system. The first six vibration modes are shown in Figure 12. The first vibration mode is the first symmetric mode (denoted as 1S) having frequency $\omega_p=9.902\text{sec}^{-1}$.

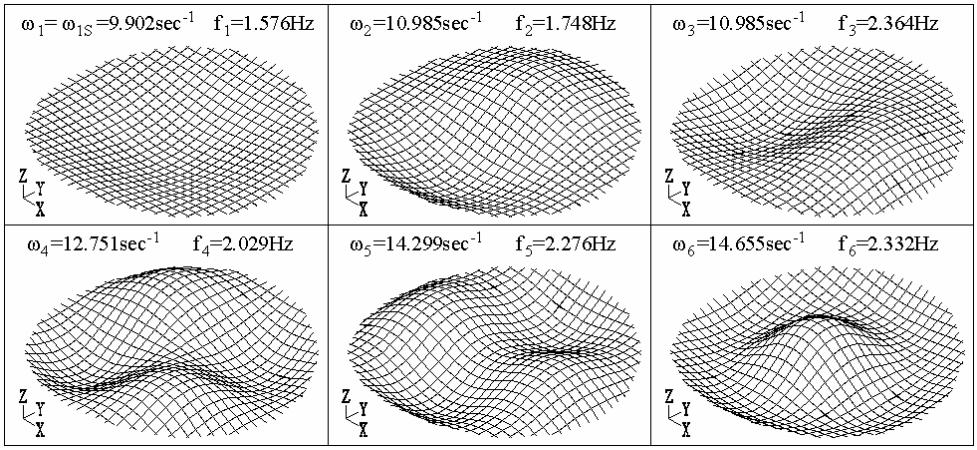

Figure 12: The first six vibration modes of the prototype

According to similarity relation (9) the natural frequency of the model, calculated as ω_m=8.22sec^{-1}, should be equal to the prototype's one. The natural frequency of mode 1S, obtained by the equivalent SDOF model, is 17% smaller than the one calculated by modal analysis of the MDOF system. The difference is rather large, because the difference between the model and the prototype, regarding the number of cables is also large. Nevertheless, this method is not used to calculate with accuracy the eigenfrequency, the maximum deflection or the cable tension of the prototype, but it is proposed to detect the occurrence of nonlinear phenomena.

5.3.2. Fundamental resonance

Accounting for fundamental resonant phenomena the load amplitude of the harmonic uniform load is chosen in section 5.2.2, equal to $(P_0)_p$=1.30kN. The load frequency varies between $0.90\omega_p$ and $1.30\omega_p$. The damping ratio, according to similarity relation (11), is considered equal to $\zeta_p=\zeta_m=\zeta$=2%. The amplitude of the steady state response for the central node of the MDOF prototype with respect to the ratio of the loading frequency over the eigenfrequency, is plotted in Figure 13. In the same diagram the response of the SDOF model of Figure 3 is also illustrated for comparison reasons. According to similarity relation (8), the nodal dynamic deflection of the prototype should be equal to the one of the model. For frequency ratios between Ω/ω_p=0.90 and Ω/ω_p=1.10, the error of the calculation is not more than 10%, which is considered as satisfactory. After the peak amplitude and as the frequency ratio increases, the error increases too, arising at 45% for Ω/ω_p=1.30. This occurs because the sixth mode of the MDOF system is another symmetric mode, having a natural frequency equal to ω_6=14.655sec^{-1}=$1.48\omega_1$=$1.48\omega_p$. Thus, as the loading frequency approaches the frequency of this mode, the amplitude increases, leading to a fundamental resonance for the sixth mode. Using the equivalent SDOF model, which has a unique frequency, is not possible to predict this second fundamental resonance.

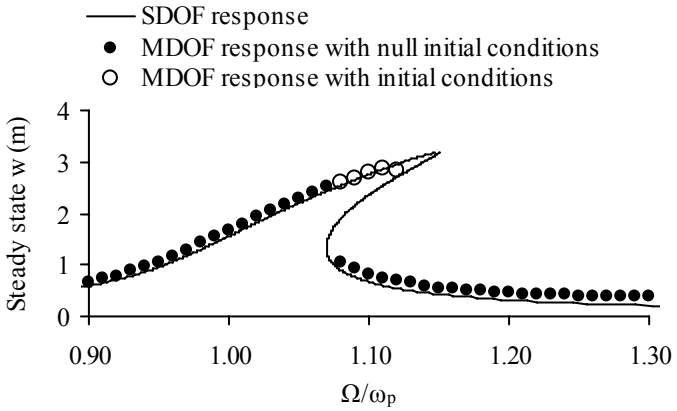

Figure 13: Fundamental resonance: response curve of the MDOF prototype for load amplitude $(P_0)_p$=1.30kN

The bending of the response curve for the MDOF system is obvious from the diagram of Figure 13. If null initial conditions are assumed, by means of deformation and velocity on every node, when the frequency ratio is Ω/ω_p=1.07 the steady state amplitude is 2.52m, while for Ω/ω_p=1.08, the amplitude drops suddenly to 1.06m, verifying the jump phenomenon. However, if initial conditions are assumed, the amplitude of the steady state deflection for Ω/ω_p=1.08 is 2.62m, verifying that the dynamic response of the MDOF prototype depends on the initial conditions. The initial conditions are deformations and velocities with respect to the three global axes, applied on every node, taken from the response of the MDOF system for Ω/ω_p=1.07 (Figure 14).

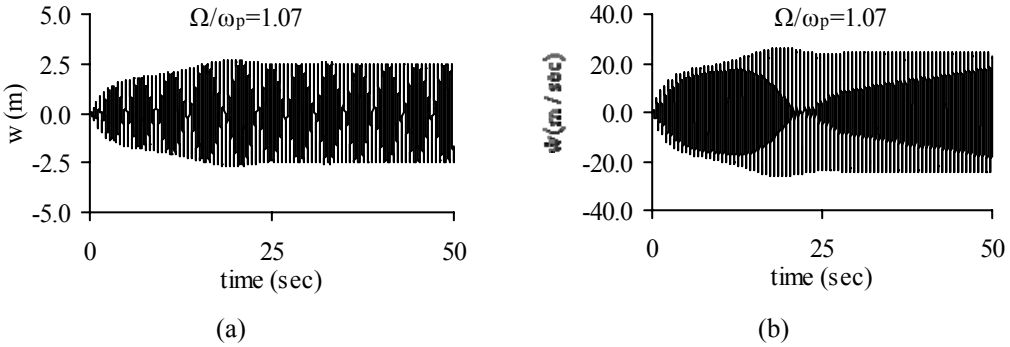

Figure 14: Time history response of the central node for Ω/ω_p=1.07: a) deflection diagram and b) vertical velocity diagram

At time t=49.58sec, both vertical displacement and velocity are considerable (Figure 15), thus the deflection (Figure 16) and the velocity (Figure 17) at that time are chosen as initial conditions for the next frequency step. The time history diagrams for Ω/ω_p=1.08, for these two cases of initial conditions, are plotted in Figure 18, showing the different response amplitudes.

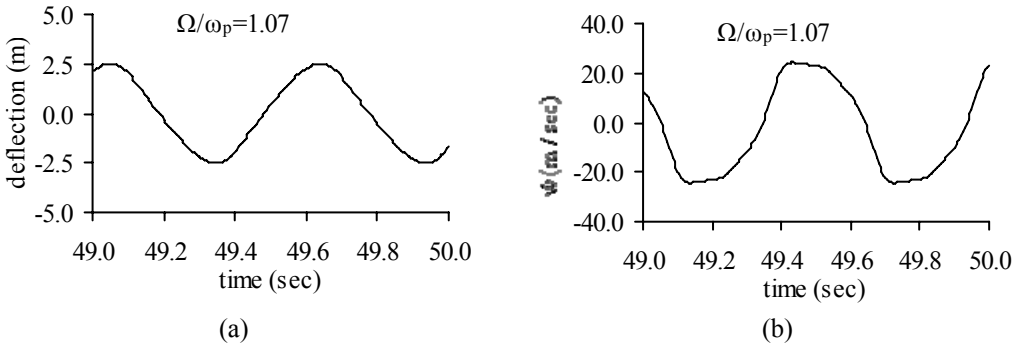

Figure 15: Time history response of the central node for Ω/ω_p=1.07 (detail): a) deflection diagram and b) vertical velocity diagram

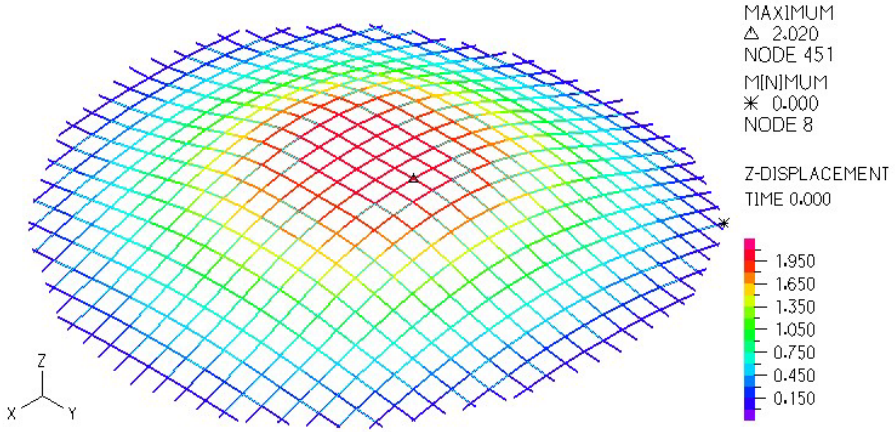

Figure 16: Vertical initial deflection for Ω/ω_p=1.08

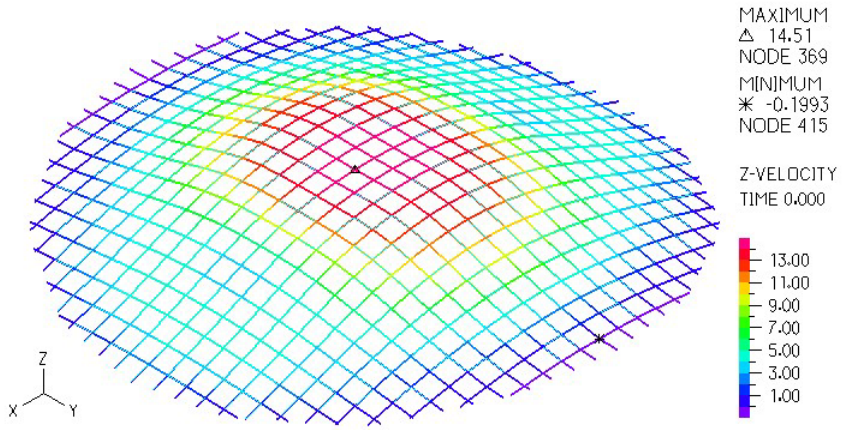

Figure 17: Vertical initial velocity for Ω/ω_p=1.08

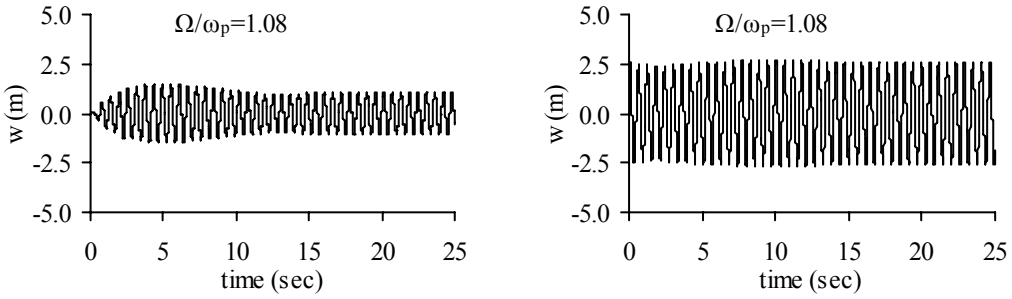

Figure 18: Time history diagrams of the central node deflection for Ω/ωp=1.08: a) with null initial conditions, b) with initial displacement and velocity

These phenomena, namely the maximum steady state amplitude occurring for frequency ratio larger than 1, leading to the bending of the curve, the jump and the multiple response amplitudes dependent on the initial conditions, also verified by the numerical simulation, confirm the intense nonlinearity of the MDOF cable net, which was predicted by the SDOF model.

5.3.3. Superharmonic resonance

In case of superharmonic resonance the load amplitude for the MDOF prototype is chosen in section 5.2.3, equal to $(P_0)_p$=14kN. The load frequency varies between $0.30\omega_p$ and $0.60\omega_p$. The amplitude of the steady state response for the central node of the MDOF prototype with respect to the frequency ratio, and the response of the equivalent SDOF model of Figure 4, are plotted together in Figure 19. The steady state amplitudes, estimated by the method of the SDOF model, are between 25% and 48% larger than the ones obtained by numerical analysis. This estimation cannot be considered as satisfactory. On the other hand, the peak amplitude for frequency ratio Ω/ω_p=0.36, predicted by the equivalent SDOF model, is verified for the prototype, confirming the occurrence of the 3:1 superharmonic resonance for the first symmetric mode.

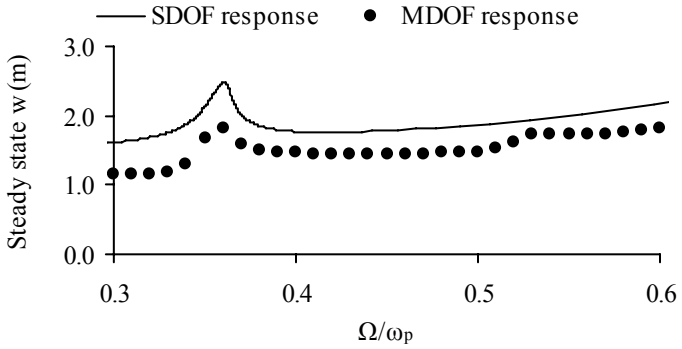

Figure 19: Superharmonic resonance: response curve of the MDOF prototype for load amplitude $(P_0)_p$=14kN

In Figure 20 the response of the central node is depicted by means of time history diagram and response spectrum, verifying this nonlinear resonance. The steady state response, obtained after 20sec, is an oscillation of at least two different frequencies. This is also illustrated in the response spectrum, in which two peaks are noted for frequencies 0.56Hz ($3.52sec^{-1}$), which is almost equal to the loading frequency ($\Omega=0.36\cdot9.902sec^{-1}=3.56sec^{-1}$) and

1.68Hz (10.56sec^{-1}), which is almost equal to the eigenfrequency of the first symmetric mode ($\omega_1=\omega_{1S}=\omega_p=9.902\text{sec}^{-1}$).

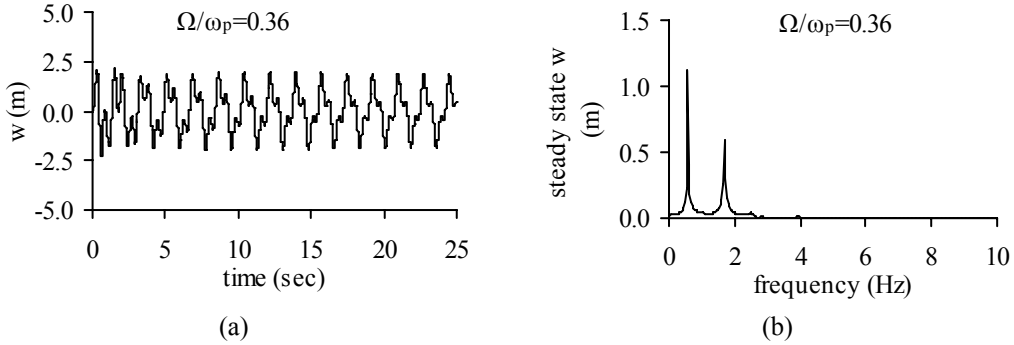

Figure 20: Response diagrams of the central node deflection for $\Omega/\omega_p=0.36$: a) time history diagram, b) response spectrum

In Figure 19, a second peak of the amplitude is observed for frequency ratio $\Omega/\omega_p=0.53$ for the MDOF system, which corresponds to a 2:1 superharmonic resonance for the same mode. In this case, the loading frequency is $\Omega=0.53\cdot\omega_p=5.52\text{sec}^{-1}=0.36\omega_6$, where ω_6 is the eigenfrequency of the sixth mode equal to $\omega_6=14.655\text{sec}^{-1}$. Hence, this second peak indicates also a 3:1 superharmonic resonance for the sixth mode being the second symmetric mode of the system.

In Figure 21a, the time history diagram of the central node deflection is plotted. In Figure 21b, the response spectrum of the central node deflection illustrates that the oscillation of the central node is characterized by three frequencies: at 0.84Hz, corresponding to 5.28sec^{-1}, which is very close to the loading frequency ($\Omega=0.53\cdot\omega_p=5.25\text{sec}^{-1}$), at 1.72Hz (10.81sec^{-1}), being close to the eigenfrequency of the first symmetric mode ($\omega_1=\omega_{1S}=\omega_p=9.902\text{sec}^{-1}$) and at 2.52Hz (15.83sec^{-1}), which is close to the eigenfrequency of the second symmetric mode ($\omega_6=14.655\text{sec}^{-1}$). Thus, both modes are activated in this case and the occurrence of the 3:1 and 2:1 superharmonic resonance for the first and the second symmetric mode, respectively, is verified. With the equivalent SDOF model having only one frequency, it is not possible to predict this second superharmonic resonance for the mode of higher order. In addition, the SDOF model, having only a cubic nonlinear term, cannot detect 2:1 superharmonic resonances.

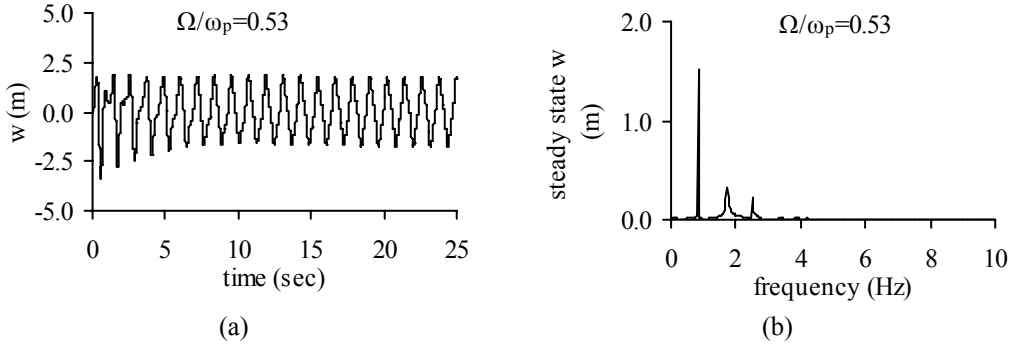

Figure 21: Response diagrams of the central node deflection for $\Omega/\omega_p=0.53$: a) time history diagram, b) response spectrum

5.3.4. Subharmonic resonance

Based on the parametric analysis of section 5.2.4, assuming a load amplitude on every node equal to $(P_0)_p$=51kN, with a load frequency equal to $\Omega=3.44\omega_p$, and an initial deflection and velocity on every node, so that the ones for the central node are 2.30m and 16m/sec, respectively, subharmonic resonance should be developed, but before the first cycle of the oscillation concludes, cable tensile failure occurs. The same also occurs for load amplitude $(P_0)_p$=56kN, loading frequency $\Omega=3.32\omega_p$ and initial conditions, corresponding to a deflection and velocity for the central node, 1.48m and 16m/sec, respectively (Figure 22). For smaller load amplitudes, a larger initial deflection is required, and for smaller initial deflection, a larger load amplitude can cause a subharmonic resonance. Both cases lead to cable tensile failure. Thus, for this cable net, it is impossible for the subharmonic resonance to evolve, because the large load amplitude and the large initial conditions required for such a resonance, cause cable tensile failure as soon as the vibration starts.

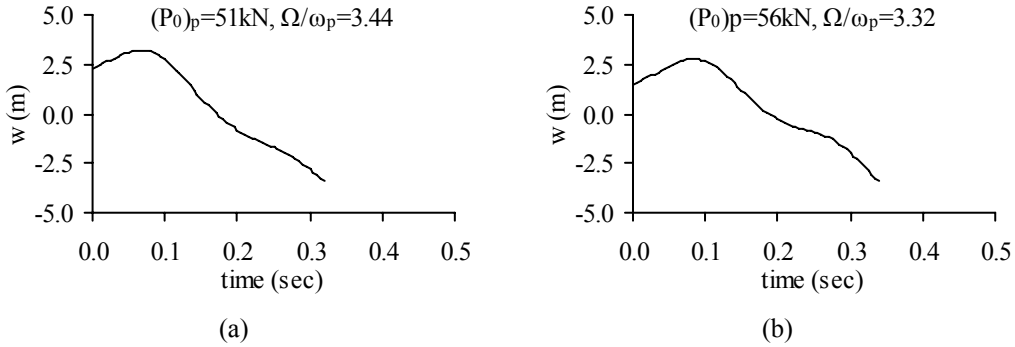

Figure 22: Time history response of the central node for: a) $(P_0)_p$=51kN and Ω/ω_p=3.44 b) $(P_0)_p$=56kN and Ω/ω_p=3.32

6 EVALUATION OF THE METHOD

The pros of the proposed method are the following:

- The computational time required to solve the equation of motion and have an assessment of the response of the MDOF system is minimal.
- The intensity of the geometrical nonlinearity of the MDOF system can be estimated very satisfactorily, by means of the bending of the response curve, the jump phenomena and the existence of double response amplitudes due to the initial conditions.
- The loading frequency detuning, for which nonlinear resonances for the first symmetric mode occur, can be estimated with good accuracy.

The cons of this method are the following:

- The equivalent SDOF model, having only one eigenfrequency and eigenmode, cannot detect resonances for higher modes for a MDOF cable net.
- The equivalent SDOF model, having only a cubic nonlinear term, cannot predict 2:1 superharmonic or 1:2 subharmonic resonances for the large system.
- The analytical solution of the SDOF cable net is given for the vertical load applied on the central node, causing a vertical vibration. Thus, only the oscillation amplitude of the central node of the MDOF system can be estimated.
- In addition, this vertical motion corresponds to the first symmetric mode of the cable net. Hence, the method of the equivalent SDOF model cannot be used to estimate the response

of the MDOF cable net for other modal shapes, or for other spatial loading distributions, such as anti-symmetric ones about one or two horizontal axes.

- The analytical solution of the SDOF cable net gives the steady state amplitude of the response but not the maximum transient response, for which a cable tensile failure is possible to occur, before the steady state response is reached.

7 SUMMARY AND CONCLUSIONS

A method of an equivalent single-degree-of-freedom cable net is introduced, in order to predict the nonlinear dynamic response of a multi-degree-of-freedom cable net. The geometrical and mechanical characteristics of the large cable net are transformed to the corresponding ones of the small cable net, using similarity relations. The analytical solution of the SDOF model is explored, in order to detect nonlinear phenomena, such as the bending of the response curve, the occurrence of superharmonic and subharmonic resonances, jump phenomena and the double response amplitudes with respect to the initial conditions. The results of the SDOF model, by means of the maximum load, the maximum deflection and the loading frequency, are transformed to the ones of the MDOF system, by using the inverse similarity relations. Conducting nonlinear dynamic analyses and numerical simulation of the MDOF cable net, the nonlinear phenomena are verified.

This investigation verifies that the saddle form cable nets have cubic nonlinearities, but also quadratic ones. Near resonances, although damping exists, a small change of the loading frequency may cause large difference in the oscillation amplitude. The initial conditions influence significantly the response of the cable net, as occurs in nonlinear systems. Jump phenomena and superharmonic resonances are also confirmed. Concerning the subharmonic resonances, it is very difficult to detect them for a MDOF system, because they require specific load amplitude, load frequency and initial conditions. It is impossible to know which load amplitude and frequency and which initial deflection and velocity can cause this kind of nonlinear resonance, because no analytical solutions are available. The investigation of the SDOF model showed that subharmonic resonances may occur under certain conditions, but for the MDOF they are difficult to exhibit, because the large initial conditions and the large load amplitude required for this phenomenon lead to cable tensile failure at the beginning of the vibration.

The numerical investigation of the overall nonlinear dynamic behaviour of a MDOF cable net system is a time consuming procedure. It requires much computational time and a large number of nonlinear time history analyses, for different load amplitudes and for very small time steps and frequency steps. This method, estimating the loading amplitudes and frequencies for which nonlinear phenomena take place, can be a very useful guideline for the design of such cable structures.

REFERENCES

[1] G. Kerschen, K. Worden, A. F. Vakakis and J. Golinval, Past, present and future of nonlinear system identification in structural dynamics, *Mechanical Systems and Signal Processing*, **20**, 505-592, 2006.

[2] G. C. Mays and P. D. Smith, *Blast effects on Buildings*. Thomas Telford, England, 1995.

[3] C. M. Morison, Dynamic response of walls and slabs by single-degree-of-freedom analysis – a critical review and revision, *International Journal of Impact Engineering*, **32**, 1214-1247, 2006.

[4] S. Resemini, S. Lagomarsino and S. Giovinazzi, Damping factors and equivalent SDOF definition in displacement-based assessment of monumental masonry structures, *1st European conference on earthquake engineering and seismology*, Geneva, Switzerland, 2006.

[5] H. N. Li, F. Wang and Z. H. Lu, Estimation of Hysteretic Energy of MDOF structures based on equivalent SDOF Systems, *Key Engineering Materials*, **340-341**, 435-440, 2007.

[6] G. E. Manoukas, A. M. Athanatopoulou and I. E. Avramidis, Static Pushover Analysis Based on an Energy-Equivalent SDOF System, *14th World Conference on Earthquake Engineering*, Beijing, China, 2008.

[7] R. Zaharia and F. Taucer, Equivalent period and damping for EC8 spectral response of SDOF ring-spring hysteretic models, *JRC Scientific and Technical Reports*, European Communities, 2008.

[8] M. Aschheim and J. Browning, Influence of cracking on equivalent SDOF estimates of RC frame drift, *Journal of Structural Engineering*, **134**, 511-517, 2008.

[9] A. J. A. Oviedo, M. Midorikawa and T. Asari, An equivalent SDOF system model for estimating the response of R/C building structures with proportional hysteretic dampers subjected to earthquake motions, *Earthquake Engineering and Structural Dynamics*, Wiley online library, 2010.

[10] E. Buckingham, On physically similar systems; Illustrations of the use of dimensional equations, *Physical Review*, **4**, 345-376, 1914.

[11] J. S. Gero, The behaviour of cable network structures, *Structures Report SR8*, University of Sydney, 1975.

[12] J. S. Gero, The preliminary design of cable network structures, *Structures Report SR9*, University of Sydney, 1975.

[13] I. Vassilopoulou and C. J. Gantes, Behaviour and preliminary analysis of cable net structures with elastic supports, *4th National Conference on Metal Structures*, Patras, Greece, **2**, 517-525, May 24-25, 2002.

[14] I. Vassilopoulou and C. J. Gantes, Behavior, Analysis and Design of Cable Networks Anchored to a Flexible Edge ring, International Association for Shell and Spatial Structures, *Symposium on Shell and Spatial Structures from Models to Realization (IASS2004-Symposium Montpellier)*, Montpellier, France, Extended Abstract, pp. 212-213, September 20-24, 2004.

[15] I. Vassilopoulou and C. J. Gantes, Cable nets with elastically deformable edge ring, *International Journal of Space Structures*, **20**, 15-34, 2005.

[16] I. Vassilopoulou and C. J. Gantes, Similarity relations for nonlinear dynamic oscillations of a cable net, *1st ECCOMAS Thematic Conference on Computational Methods in Structural Dynamics and Earthquake Engineering (COMPDYN 2007*), Rethymno, Crete, Greece, abstract pp. 373, June 13-16, 2007.

[17] A. K. Chopra, *Dynamics of structures, Theory and applications to earthquake engineering*. Prentice Hall International, Inc. U.S.A. 1995.

[18] H. A. Buchholdt, *An introduction to cable roof structures, 2nd Edition.* Thomas Telford, England, 1999.

[19] A. Nayfeh and D. T. Mook, *Nonlinear Oscillations*. John Wiley & Sons, Inc. U.S.A., 1979.